

# Fault Diagnosis in Bipolar HVDC Systems Based on Traveling Wave Theory by Monitoring Data From One Terminal

Júlio César Cândido Vieira, Damásio Fernandes Júnior, Washington Luiz Araújo Neves, Felipe Vigolvino Lopes

**Abstract**—This paper proposes a method for detecting, classifying and locating incident faults on transmission line (TL) of a bipolar HVDC system. This method is based on the traveling waves theory and uses the redundant discrete wavelet transform to filter voltage signals monitored at only one system terminal. The model represents the Brazilian HVDC system of the Madeira River, which is simulated in the Alternative Transient Program (ATP). Different fault scenarios are analyzed, being generated by varying type, resistance and fault location. Moreover, in order to make the simulation more realistic, the TL is modeled based on frequency dependent parameters. Thereby, the impacts of line parameter uncertainties and transient attenuation on the proposed method are analyzed. From the obtained results, it is concluded that the method correctly detects all fault types through the use of a self-adaptive detection threshold. Furthermore, it is verified that the self-adaptive threshold detects the fault times instants with an efficiency superior to the fixed threshold. In the classification step, all faults were correctly classified through rules elaborated based on the voltage variation level. Finally, the total average errors of fault location represents only 0.047% of the TL extension. Moreover, it is verified that fault location errors for pole:pole faults were inferior to those obtained for pole:ground faults, being the efficiency of the method inversely proportional to the fault resistance.

**Keywords**—Fault diagnosis, HVDC systems, traveling waves theory, wavelet transform.

## I. INTRODUCTION

**I**N recent decades, electrical power systems have evolved in complexity and size, which has led the distance between generating plants and main consumer centers to increase. Thus, several researches have focused on the development of solutions to allow the transmission of bulk power over long distances [1]. Among the possible solutions, the High Voltage Direct Current (HVDC) transmission system stands out.

The constant technological advances in power electronics have enabled the use of direct current to transmit electrical energy over long distances at lower costs and no reactive compensation throughout the lines [2]. Due to their long extensions, an HVDC TL cross distinct and unpredictable environments and, consequently, are more susceptible to

disturbances. Therefore, a quick and accurate diagnosis (detection, classification and location) of disturbances is of paramount importance to ensure the restoration of system operation.

In the context of transmission systems, traveling wave (TW)-based fault location methods have attracted the interest from utilities, mainly because they are immune to sources of errors that usually affect traditional techniques based on the fundamental component analysis [3]. Moreover, TW-based methods have been taken as suitable solutions for HVDC systems, mainly due to their structure simplicity and to the fact that converter stations constrain the fault-induced TWs into the monitored line [4].

Depending on the number of monitored stations, TW-based fault location methods can be classified in one or two-terminal. The classical one and two-terminal fault location methods were applied in HVDC systems in [5] and [6], respectively. Besides the classical methods, new alternative methodologies have been developed in order to eliminate the dependence of the line parameters, propagation velocity of TWs and need for synchronized data [7]–[9].

The main step of TW-based algorithms is the fault-induced transient detection. It allows the computation of the time at which traveling waves due to faults reach the monitored line terminals. Among the techniques used to filter the signal, wavelet transforms have great prominence due to its simultaneous time and frequency localization capabilities [10], [11]. However, in real fault location applications, the coefficients generated by the wavelet transform must be compared to a threshold in order to detect the transient time instant. Thus, its performance depends on the chosen threshold.

Several transient detection techniques are based on the hard thresholding [12], where the first fast-rising point used to detect transients is defined as the sample whose coefficient exceeds the hard threshold for the first time among all samples. The instant at which the first fast-rising point occurs nearly coincide with the time when transient starts. However, these techniques are sensitive to electrical noises and other variations. Thus, first fast-rising point may be identified erroneously, and the reliability of the transient detection can be compromised [13]. In order to overcome this problem, a self-adaptive threshold is proposed here to detect the transient inception times.

Despite the several advances in TW-based fault location methods applied to HVDC systems, techniques regarding the

---

Júlio César, Damásio Fernandes and Washington Neves are with the Department of Electrical Engineering of Federal University of Campina Grande (UFCG), 58429-900 Campina Grande-PB, Brazil. (e-mail: julio.vieira@ee.ufcg.edu.br, damasio@dee.ufcg.edu.br, waneves@dee.ufcg.edu.br).

Felipe Lopes is with the Department of Electrical Engineering of Federal University of Paraíba (UFPB), 58051-900 João Pessoa-PB, Brazil. (e-mail: felipelopes@cear.ufpb.br).

Paper submitted to the International Conference on Power Systems Transients (IPST2023) in Thessaloniki, Greece, June 12-15, 2023.

complete fault diagnosis (detection, classification and location) are scarce in the literature. In this context, this paper presents a method to detect, classify and locate faults in a bipolar HVDC system using voltage data monitored only at one system terminal.

The proposed method is based on TWs and uses the Redundant Discrete Wavelet Transform (RDWT) to filter the monitored signals. The detection of fault instants is performed through a comparative analysis between the absolute values of RDWT coefficients obtained from voltage signal with a self-adaptive threshold. In order to evaluate the method performance, simulations of various scenarios of faults on TLs of the Brazilian HVDC system of Madeira River are performed. Such system was modeled in the Alternative Transient Program (ATP) software and the fault cases were generated by varying the location, resistance and fault type.

## II. FAULT LOCATION BASED ON TRAVELING WAVES

### A. Traveling Wave Theory

The traveling wave theory is characterized by the propagation of electromagnetic waves of voltage and current in both directions of a TL. Such waves are generated through abrupt changes in the system and propagates as electromagnetic transients. Moreover, the TWs can be reflected and refracted at system discontinuities such as the fault point and TL terminals [14].

In order to illustrate the propagation of TWs, Fig. 1 shows the Bewley diagram, in which the TWs propagation is characterized in time-space domain.

According to Fig. 1: the first incident TWs reach terminals rectifier and inverter at the instants  $t_{R1}$  and  $t_{I1}$ , respectively; TWs reflected from the fault point reach terminals rectifier and inverter at the instants  $t_{R2}$  and  $t_{I2}$ , respectively, and TWs refracted from the fault point arrive at terminals rectifier and inverter at the instants  $t_{I1r}$  and  $t_{R1r}$ , respectively.

Assuming that monitoring devices are installed at both system terminals, the two-terminal method can be applied

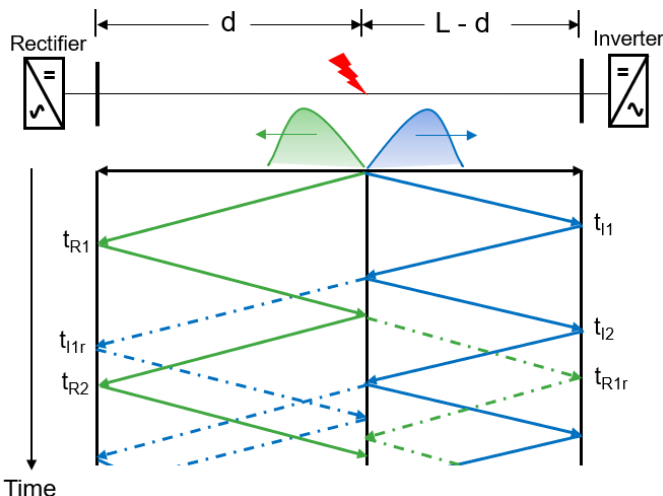


Fig. 1. Bewley diagram of traveling waves generated from the fault point.

by obtaining the instants  $t_{R1}$  and  $t_{I1}$ . However, to properly identify these time instants, a synchronized communication channel is necessary. This fact represents an obstacle to application of two-terminal methods in systems without a common time reference or when the time reference signal is lost [15]. Due to this, the one-terminal method is used to estimate the fault position in this paper.

Considering the rectifier as a monitoring terminal, the one-terminal method can be applied by (1):

$$d = \frac{(t_{R2} - t_{R1}) \cdot v_p}{2}, \quad (1)$$

where  $v_p$  is TWs propagation velocity.

From (1), it can be verified that in one-terminal method, as only one terminal is monitored, the time synchronization between the devices is not required. This represents the main advantage of applying the one-terminal methods. On the other hand, due to the successive TWs reflection and refraction processes, the detection of  $t_{R2}$  can be confused with the instants  $t_{I1r}$  or  $t_{I2r}$ , depending on the fault location. In order to avoid such errors, TWs polarities are used in the detection process in this work, as explained in next sections.

### B. Traveling Waves Arrival Time Detection

In TW-based fault location methods, the filtering of the analyzed signals is of paramount importance to ensure the method reliability. Among the techniques used to perform such filtering, discrete wavelet transforms (DWT) have great prominence due to its capability of analyzing a signal in different time and frequency scale [10].

The DWT is composed by low- and high-pass filters to divide the frequency-band of the input signal into low- and high-frequency components (scaling and wavelet coefficients). This operation may be repeated recursively, feeding the low-pass filter output into another identical filter pair, decomposing the signal into scaling and wavelet coefficients at various scales [16].

The redundant discrete wavelet transform (RDWT) is a DWT variant. However, in contrast to the DWT, there is no down-sampling in RDWT (time-invariant transformation) [17]. Consequently, transients caused by faults can be detected faster by means of the RDWT. Due to this, the RDWT is used in this work to filter the analyzed signals.

Based on [18], the RDWT wavelet coefficients are calculated as demonstrated in (2). The calculation considers Haar as mother wavelet due to its simplicity application and ability to analyze signals with sudden transitions:

$$c(t) = \frac{x(t) - x(t - \Delta t)}{2\sqrt{2}}, \quad (2)$$

where  $c(t)$  and  $x(t)$  represent the calculated RDWT coefficient and signal analyzed at instant  $t$ , respectively. The parameter  $x(t - \Delta t)$  represents the signal analyzed at instant  $t - \Delta t$ , where  $\Delta t$  is the sampling frequency.

The RDWT coefficient represents the variation of the analyzed signal between two consecutive instants, being equivalent to the time derivative process. The units of this coefficient can be represented in absolute values.

Finally, the detection of wave arrival time instants at the monitoring terminal occurs by comparing the absolute value of the coefficient calculated via (2) with a self-adaptive detection threshold, which is explained in the next sections.

### III. HVDC SYSTEM MODEL

#### A. Modeled System

The HVDC system used in this study was modeled using the ATP/ATPDraw in [19] and represents the Madeira River HVDC system. The system is composed by two bipoles (3150 MW and  $\pm 600$  kV) that interconnect the Brazilian converters stations of Coletora Porto Velho and Araraquara 2 through a transmission line of 2450 km long and rated current of 2625 A. All the components of the HVDC system (transmission line, AC and DC filters, inverters, smoothing reactor and transformers) are modeled in ATP/ATPDraw. The Fig. 2 presents a single-line diagram of the HVDC system and its components.

The original HVDC transmission line model adopted in [19] considers frequency independent line parameters. However, the frequency dependent line parameters model is more accurate for TWs studies, as it results in more critical TWs attenuation and dispersion [20]. Therefore, in order to make the simulation more realistic, the frequency dependent line model was used. To do so, the transmission tower geometry and conductor specifications presented on Fig. 3 were modeled using the JMarti model in ATP/ATPDraw [21].

#### B. Simulations

The TL faults of the analyzed system were simulated in ATP/ATPDraw and a sampling frequency equal to 1 MHz was emulated. This sampling frequency value was used in order to represent the high resolution rates of intelligent electronic devices in real electrical power systems.

The different fault characteristics were generated by the variation of the location, resistance and fault type. The values of the fault distance in relation to the rectifier terminal were varied between 25 km to 2425 km, with steps of 50 km, which represents approximately 2% of the TL total length. The fault resistance was varied between 0.1 and 500  $\Omega$  in order to evaluate the fault impedance influence on the method efficiency. The analyzed fault types were: pole+:ground, pole-:ground and pole:pole. In Table I all evaluated fault cases are summarized, totaling 1764 different scenarios.

TABLE I  
FAULT CASES.

Local (km)	Type	Resistance ( $\Omega$ )
25, 75, ..., 2.375, 2.425	Pole+:Ground, Pole-:Ground, Pole:Pole	0,1; 1; 5; 10; 30; 50; 100 150; 200; 300; 400; 500

### IV. PROPOSED METHOD

It is proposed here to implement a detection, classification and location method of incident disturbances on HVDC TL. This method uses voltage data monitored at one of the HVDC terminals and considers the rectifier as the reference terminal.

The data simulated in ATP software are exported to Matlab<sup>®</sup> program. The methodologies and rules used to carry out each step of the fault diagnosis procedure are performed in Matlab<sup>®</sup> and they will be presented in next subsections.

#### A. Detection

For all fault scenarios shown in Table I, the voltage data monitored at rectifier terminal poles are analyzed in order to calculate the redundant discrete wavelet transform coefficients using (2).

The transient detection process is based on comparing the RDWT coefficients absolute values with a self-adaptive detection threshold, which is composed of two parameters. The first parameter to be calculated is the standard deviation of the voltage signal ( $\sigma_V$ ), which must be obtained in a sample interval in which the system is operating in steady state.

$$\sigma_V = \sqrt{\frac{\sum [(V(t) - \mu_V)^2]}{n}}, \quad (3)$$

where  $V(t)$  is the voltage value for instant  $t$ ,  $\mu_V$  is the average of voltage values and  $n$  is a number of samples in considered interval.

The second parameter used to calculate the self-adaptive threshold is the system characteristic factor ( $F_{CS}$ ). This parameter is calculated by the ratio between the maximum and average value of the RDWT coefficients modules. It is noteworthy that the characteristic factor is obtained considering the same time interval used to calculate  $\sigma_V$ .

With the parameters  $\sigma_V$  and  $F_{CS}$ , the proposed self-adaptive detection threshold ( $\rho$ ) can be obtained:

$$\rho(t) = (|c(t - \Delta t)| + F_{CS}) \cdot \sigma_V, \quad (4)$$

where  $c(t - \Delta t)$  is the calculated RDWT coefficient at instant  $t - \Delta t$ . The parameter  $\Delta t$  represents the sampling time period, which results in a sampling frequency equal to 1 MHz in this study.

As presented, the proposed threshold is self-adaptive, and follows the progression of standard deviation itself, considering a previously defined interval. In order to illustrate the detection process, the RDWT coefficients of the voltage data for a pole+:ground fault are shown in Fig.4.

Note that the self-adaptive threshold has its value modified as a function of the instant of time prior to that of the analyzed sample. Therefore, the threshold calculated in (4) must be compared with the absolute value of the RDWT coefficient at instant  $t$ . If the value of  $|c(t)|$  is greater than the threshold, the transient is detected.

#### B. Classification

The fault classification is performed through rules formulated based on monitored voltage signals analysis. In order to illustrate the classification process, Fig. 5 presents the voltage data at rectifier poles for pole+:ground, pole-:ground and pole:pole faults, considering a fault resistance of 100  $\Omega$ .

Based on analysis of Fig. 5, it is verified that fault involving one of the poles (positive or negative) and ground produces a severe voltage dip only at the faulted pole. Meanwhile, a

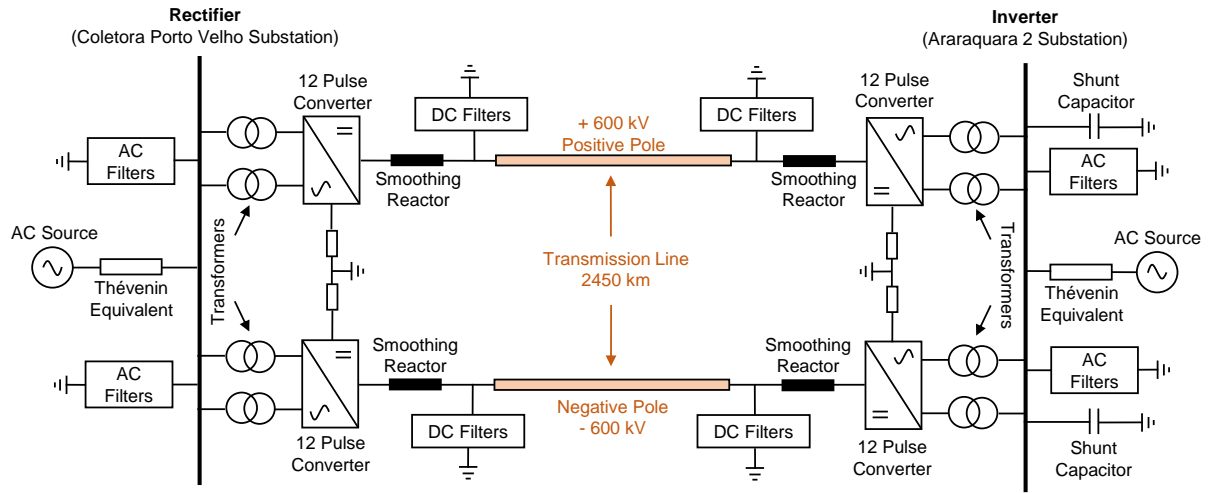


Fig. 2. Diagram of modeled system that represents the Madeira River HVDC system.

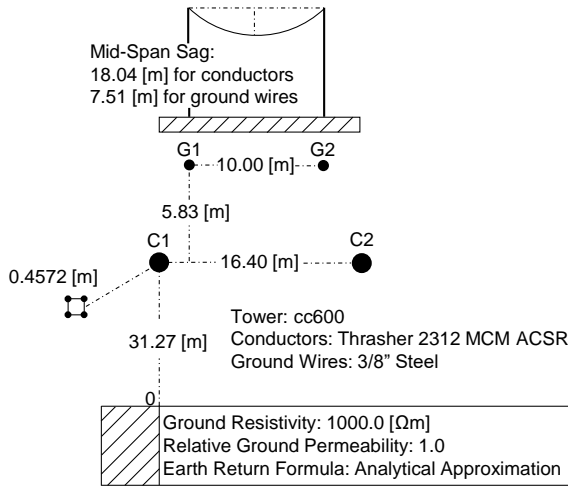


Fig. 3. HVDC tower parameters presented in [19].

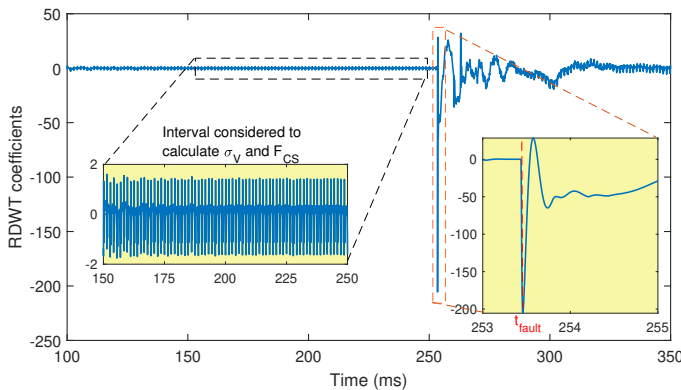


Fig. 4. Fault detection process.

pole:pole fault produces a voltage dip at both system poles. Thus, rules were formulated to classify the faults using the voltage data variations, as shown next.

- 1) Obtain the voltage value on positive ( $V_{pos_{fault}}$ ) and negative ( $V_{neg_{fault}}$ ) pole at fault detection time;
- 2) Obtain the minimum voltage value on positive pole

( $V_{min_{pos}}$ ) and the maximum voltage value on negative pole ( $V_{max_{neg}}$ ) of the rectifier after the fault detection time;

- 3) Calculation of the maximum voltage variation on positive ( $\Delta V_{pos} = |V_{pos_{fault}} - V_{min_{pos}}|$ ) and negative ( $\Delta V_{neg} = |V_{neg_{fault}} - V_{max_{neg}}|$ ) pole;
- 4) Check whether  $\Delta V_{pos}$  is greater than  $\Delta V_{neg}$ ;
- 5) If item 4 is true, verifies if  $\Delta V_{neg}$  is less than  $0.3 \cdot \Delta V_{pos}$ . If this condition is satisfied, it is concluded that fault is pole+:ground;
- 6) If item 4 is false, verifies if  $\Delta V_{pos}$  is less than  $0.3 \cdot \Delta V_{neg}$ . If this condition is satisfied, it is concluded that fault is pole-:ground;
- 7) If items 5 and 6 are false, it is concluded that fault is pole:pole.

In steps 5 and 6, a multiplier factor equal to 0.3 is used. This value represents the percentage of voltage variation between the positive and negative pole and was chosen based on the classification errors analysis for factors with values from 0.1 to 0.9. The value that presented the best efficiency rate in the classification of faults was 0.3. Thus, this value is considered in this study. The choice of this factor depends on the system characteristics, being thus a method setting.

### C. Location

Based on Fig. 2, it is verified that the TL terminations of the analyzed HVDC system are composed by the smoothing reactor and DC filters, which are modeled by an association of resistors, capacitors and inductors. Through the DC filter analysis, it was verified that the TL terminations present predominantly capacitive impedance. Thus, for high frequency phenomena, such as the occurrence of TWs, the TL terminal impedance is much smaller than TL characteristic impedance. This occurs because the impedance of the capacitive termination is inversely proportional to the frequency.

As the TL terminations of the analyzed HVDC system are predominantly capacitive, the reflection coefficient polarity at TL terminations for voltage waves is negative [22]. In this

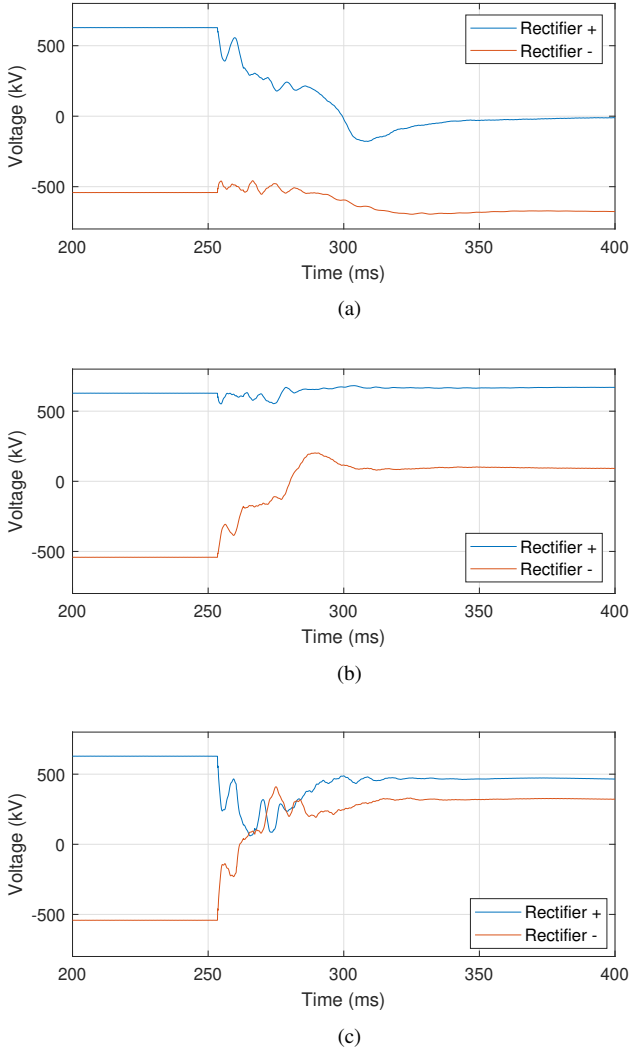


Fig. 5. Rectifier poles voltages for a fault a) pole+:ground, b) pole-:ground and c) pole:pole.

case, the TL terminal impedance ( $Z_T$ ) is much smaller than TL characteristic impedance ( $Z_S$ ) and the reflection coefficient is calculated as:

$$\Gamma_r = \frac{Z_T - Z_S}{Z_T + Z_S} < 0. \quad (5)$$

Moreover, the incident disturbance at TL represents a short circuit at fault point. Therefore, according to (5), the polarity of waves reflected at fault point discontinuity is also negative. Based on that, Fig. 6 presents the polarities of voltage waves at TL terminations. Thereby, the TWs polarity measured on rectifier terminal at instants  $t_{R1}$  and  $t_{R2}$  are the same.

In order to detect  $t_{R1}$  and  $t_{R2}$ , the second scale of RDWT is applied to voltage data as shown in Fig. 7. The second scale coefficients for a pole:ground fault located 775 km from the rectifier terminal are presented. By applying the self-adaptive detection threshold presented in subsection A, the instants  $t_{R1}$  and  $t_{R2}$  can be detected. In the specific case of Fig. 7,  $t_{R1} = 252.598 \mu\text{s}$  and  $t_{R2} = 257.811 \mu\text{s}$ .

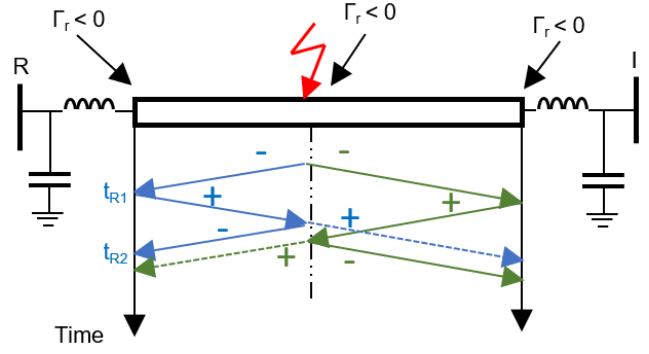


Fig. 6. Analysis of the polarities of voltage waves incident on the TL terminations.

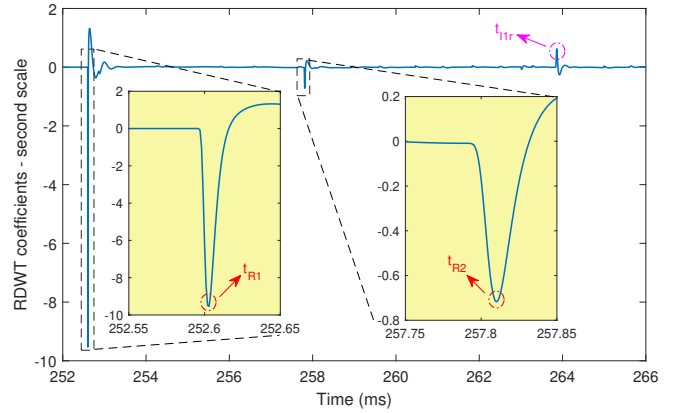


Fig. 7. Fault location process.

In order to estimate the fault location through (1), it is necessary to determine the value of TWs propagation velocity ( $v_p$ ). As the TL model is frequency dependent,  $v_p$  varies according to the dominant transient frequencies, creating line parameters uncertainties for all simulated cases. Faced with this scenario of uncertainties, the fixed propagation velocity which presented best results, diminishing differences between traveling times of rectifier was  $v_p = 297721519.14$  m/s. This velocity was estimated by applying a controlled fault and measuring the TW travel time.

## V. RESULTS

The method efficiency is evaluated through the errors obtained in each step of fault diagnosis. In detection stage, all analyzed fault cases were correctly detected through the proposed self-adaptive detection threshold. Moreover, in order to verify the performance of self-adaptive detection threshold ( $\rho(t)$ ) in relation to a fixed threshold, a comparative analysis was performed between  $\rho(t)$  and a fixed threshold equal to 2 ( $\rho_2$ ) in the  $t_{R1}$  detection process, as shown in Table II. The value of the fixed threshold was chosen based on analysis of Fig. 4, in which it is verified that, in steady state, the RDWT coefficients do not exceed the value 2. Based on Table II, the parameter  $t_{R1}$  represents the time instant detection of the first incident wave at rectifier terminal considering a self-adaptive

threshold ( $\rho(t)$ ) and a fixed threshold ( $\rho$ ). Moreover, the parameter  $\Delta t_{R1}$  represents the variation between these time instants detection.

TABLE II  
FAULT DETECTION PROCESS EVALUATION.

Fault		$t_{R1} (ms)$		$\Delta t_{R1} (\mu s)$
Type	Location	$\rho(t)$	$\rho_2$	$\rho(t) - \rho_2$
Pole+:Ground	25	250.084	250.084	0
	325	251.089	251.090	1
	625	252.095	252.097	2
	925	253.102	253.104	2
	1225	254.108	254.112	4
	1525	255.115	255.119	4
	1825	256.123	256.128	5
	2125	257.130	257.135	5
	2425	258.137	258.144	7
Pole:Pole	25	250.084	250.084	0
	325	251.089	251.090	1
	625	252.095	252.096	1
	925	253.102	253.103	1
	1225	254.108	254.110	2
	1525	255.115	255.117	2
	1825	256.123	256.125	2
	2125	257.129	257.132	3
	2425	258.136	258.140	4

According to Table II, it is verified that the use of fixed threshold causes a delay in the time instant detection ( $t_{R1}$ ) when compared to the use of self-adaptive threshold. This delay can cause errors in fault location process by TWs-based methods. Furthermore, the efficiency of the transient detection process is strongly influenced by the value of the fixed threshold adopted, thus being an adjustment factor and possible source of errors in application of methods that use the fixed threshold.

Furthermore, it is concluded that as the fault moves away from the monitoring terminal, the time delay between the detection of  $t_{R1}$  considering the self-adaptive and fixed threshold increases. This occurs because, for faults far from the monitoring terminal, the TL resistance attenuates TW amplitude more severely. Thus, the amplitude of the monitored traveling wave is smaller for faults far from the monitoring terminal when compared to those incidents close to the monitoring terminal.

In the classification stage, it was verified that all the faults cases presented in Table I were correctly classified. In this way, the efficiency of the rules elaborated based on the voltage level variation analysis is proven.

In order to analyze the technique used to estimate the fault location, the errors obtained for all types of faults analyzed are presented on Fig. 8 through a boxplot graph.

Based on Figure 8, it can be seen that the method performance is affected by the fault type variation. The general averages of the absolute errors presented in Fig. 8 are equal to 1.207 km, 1.260 km and 1.036 km for pole+:ground, pole-:ground and pole:pole faults, respectively. The general average of the errors obtained for all types of faults is equal to 1.168 km, which is equivalent to approximately 0.047% of the TL extension.

Furthermore, some outliers in the boxplot presented in Fig. 8 are verified. Such outliers result from the errors

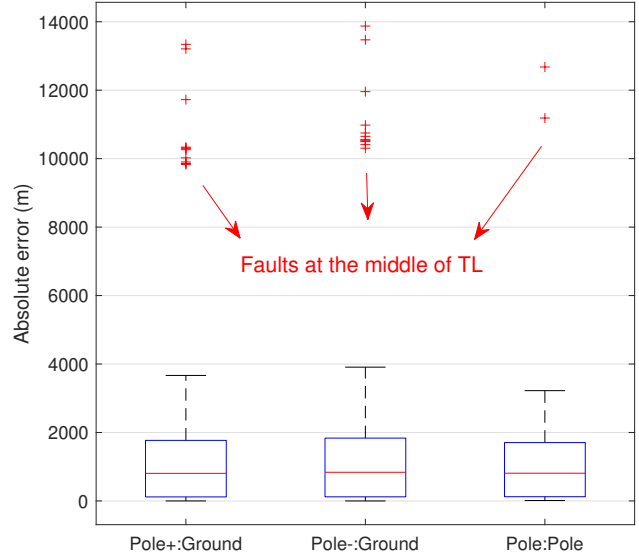


Fig. 8. Boxplots of absolute errors for each fault.

obtained for the faults exactly at the middle of the TL. This problem appears in TW-based fault location methods due to the overlapping of traveling waves that reach the monitoring terminal [14], as illustrated in Fig. 9. The RDWT coefficients for a fault distance of 1175 km, 1225 km (at TL middle) and 1275 km are presented in Fig. 9 in order to illustrate the TWs superposition.

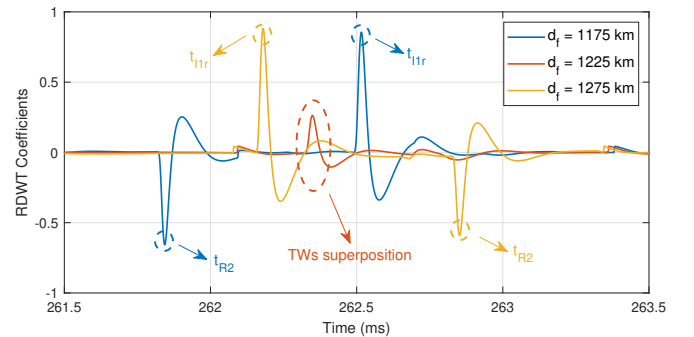


Fig. 9. RDWT coefficients for a fault's distance of 1175 km, 1225 km (at TL middle) and 1275 km.

According to Fig. 9, it is concluded that for the incident fault at TL middle, the time instants  $t_{R2}$  and  $t_{I1r}$  are approximately equal. Therefore, as the wave amplitudes at times  $t_{R2}$  and  $t_{I1r}$  are opposite, destructive interference occurs, which can cause errors in the traveling wave detection process. It should be noted that this situation is very specific and does not affect the method validity.

Furthermore, the method efficiency is also evaluated as a function of the fault resistance, as shown in Fig. 10. This graph presents the average of the location absolute errors for each type and resistance fault.

Fig. 10 demonstrates that the average location errors for pole:pole faults are smaller than those obtained for

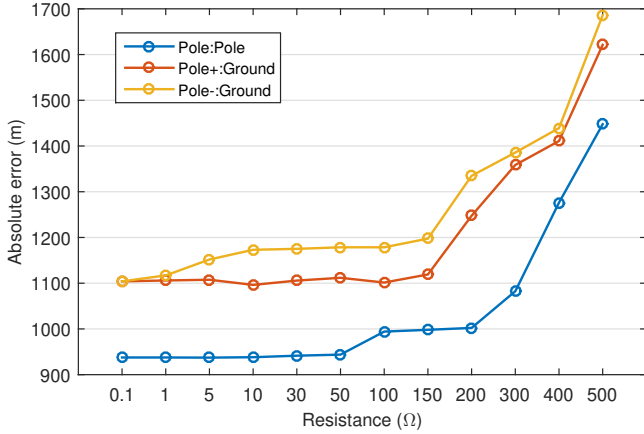


Fig. 10. Average of absolute location errors for each fault resistance.

pole:ground faults. This occurs due to the mixing mode effect, in which for pole:ground faults there is the presence of the ground mode, and, consequently, ground mode reflections and refractions can also be generated, influencing aerial mode TWs.

Furthermore, based on Fig. 10, it is concluded that the efficiency of the method is inversely proportional to the fault resistance. This result is explained by the fact that the increase in resistance attenuates the amplitude of the voltage TWs launched from the fault point [14].

According to the results presented so far, it was verified that the method proved to be more efficient in locating pole:pole faults when compared to the location of faults that involve only one pole, either the positive or negative pole. In this context, in order to evaluate this efficiency difference in more details, Fig. 11 presents a scatter plot referring to the absolute errors obtained for all cases of analyzed pole:pole and pole+:ground faults.

According to Fig. 11, it is concluded that the vast majority of errors obtained in the location of faults of the pole+:ground and pole:pole faults are smaller than 3 km. Furthermore, it is

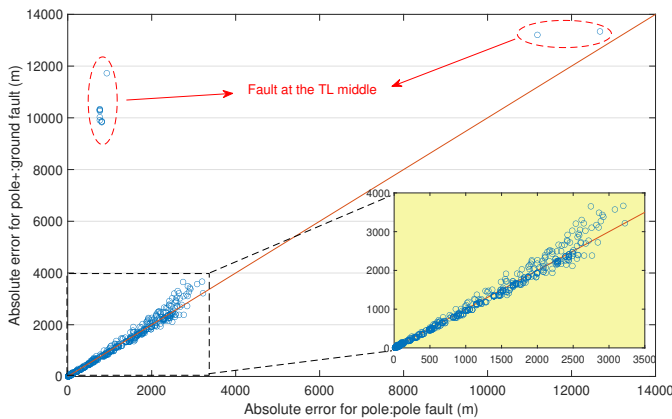


Fig. 11. Scatter plot of absolute errors obtained in locating pole:pole and pole+:ground faults.

proven that the errors obtained for the pole+:ground faults are higher than the errors obtained for the pole:pole faults for majority of cases.

Furthermore, the presence of outliers in Fig. 11 come from the errors obtained for the faults that occur at the middle of the TL, as explained early. For pole:pole faults with low fault resistance, there is no transmitted wave, which facilitates the detection process. On the other hand, for pole:ground faults, for the evaluated fault resistance, there is the presence of the transmitted wave, which causes the overlap of waves and makes the detection process more challenging.

## VI. CONCLUSIONS

This paper proposes a method of diagnosing (detection, classification and location) incident faults in the bipolar HVDC system transmission line. The method is based on traveling waves theory and uses the redundant discrete wavelet transform to filter the voltage signals monitored in only one terminal of the system.

In order to evaluate the efficiency of the proposed method, the ATP/ATPDraw software model of the Madeira River Bipole was tested through different cases of fault incidents in the transmission line. The different cases were generated by varying the type, resistance and location fault. Furthermore, the transmission line of the system was modeled based on the frequency-dependent distributed parameters in order to simulate a more realistic model capable of representing the impacts that frequency dependence imposes on HVDC systems with very long transmission lines.

From the results obtained through the evaluation of 1764 fault cases, it was verified that all faults were correctly detected and classified. This fact proves the efficiency of using the self-adaptive detection threshold and the classification rules proposed in this paper.

In the location stage, it was found that the total average of the errors obtained was equal to 1.186 km, which represents a value close to the extension of three HVDC tower spans. Furthermore, it was concluded that the method presented smaller errors in the location of pole:pole faults when compared to those obtained for pole:ground faults due to the mixing mode effect. Moreover, it was found that the efficiency of the location stage is inversely proportional to the fault resistance. This occurs due to the fact the fault resistance increasing attenuates the amplitude of the traveling waves that depart from the fault point.

Finally, it was shown that, for the analyzed system, the proposed method is 100% efficient to detect and classify faults. Additionally, it presented acceptable location errors for TW-based methods. Thus, the method is promising, especially because it only uses data monitored in one terminal, which eliminates the need for data synchronization. Moreover, as the microprocessed relays and digital fault recorders became capable to evaluate high frequency components in the megahertz range, the proposed method can be executed in real time by the implementation of the logic available in intelligent electronic devices.

## REFERENCES

- [1] F. V. Lopes, B. Küsel, and K. M. Silva, "Traveling Wave-Based Fault Location on Half-Wavelength Transmission Lines," *IEEE Latin America Transactions*, vol. 14, no. 1, pp. 248–253, 2016.
- [2] E. W. Kimbark, *Direct current transmission*, vol. 1. Wiley, 1971.
- [3] F. Lopes, E. Leite, J. P. Ribeiro, L. Lopes, and A. Piardi, "Using the differentiator-smoother filter to analyze traveling waves on transmission lines: Fundamentals settings and implementation," in *Intern. Conf. on Power Systems Transientes*, pp. 1–6, 2019.
- [4] P. Fernandes, T. Honorato, F. Lopes, K. Silva, and H. Gonçalves, "Evaluation of Travelling Wave-Based Fault Location Methods Applied to HVDC Systems," *Electric Power Systems Research*, vol. 189, p. 106619, 2020.
- [5] M. Ando, E. Schweitzer, and R. Baker, "Development and field-data evaluation of single-eng fault locator for two-terminal hvdc transmission lines part i: Data collection system and field data," *IEEE Transactions on Power Apparatus and Systems*, no. 12, pp. 3524–3530, 1985.
- [6] M. Dewe, S. Sankar, and J. Arrillaga, "The application of satellite time references to hvdc fault location," *IEEE Transactions on Power Delivery*, vol. 8, no. 3, pp. 1295–1302, 1993.
- [7] F. V. Lopes, R. L. Reis, K. M. Silva, A. Martins-Britto, E. P. Ribeiro, C. M. Moraes, and M. A. M. Rodrigues, "Past, present, and future trends of traveling wave-based fault location solutions," in *2021 Workshop on Communication Networks and Power Systems (WCNPS)*, pp. 1–6, IEEE, 2021.
- [8] F. V. Lopes, K. M. Dantas, K. M. Silva, and F. B. Costa, "Accurate two-terminal transmission line fault location using traveling waves," *IEEE Transactions on Power Delivery*, vol. 33, no. 2, pp. 873–880, 2017.
- [9] O. Naidu and A. K. Pradhan, "A traveling wave-based fault location method using unsynchronized current measurements," *IEEE Transactions on Power Delivery*, vol. 34, no. 2, pp. 505–513, 2018.
- [10] P. K. Murthy, J. Amarnath, S. Kamakshiah, and B. Singh, "Wavelet transform approach for detection and location of faults in hvdc system," in *2008 IEEE Region 10 and the Third international Conference on Industrial and Information Systems*, pp. 1–6, IEEE, 2008.
- [11] F. H. Magnago and A. Abur, "Fault location using wavelets," *IEEE transactions on power delivery*, vol. 13, no. 4, pp. 1475–1480, 1998.
- [12] S. Santoso, E. J. Powers, and W. M. Grady, "Power quality disturbance data compression using wavelet transform methods," *IEEE Transactions on Power Delivery*, vol. 12, no. 3, pp. 1250–1257, 1997.
- [13] X. Jiang, D. Wang, X. Liu, and Y. Ning, "Fault location on branched networks using a new traveling-wave algorithm," in *2016 8th International Conference on Intelligent Human-Machine Systems and Cybernetics (IHMSC)*, vol. 2, pp. 221–224, IEEE, 2016.
- [14] J. C. C. Vieira, D. F. Júnior, W. A. Neves, and F. V. Lopes, "Challenges in application of the traveling wave-based fault location methods applied to hvdc systems: Evaluation of classical one-and two-terminal methods," in *2022 20th International Conference on Harmonics & Quality of Power (ICHQP)*, pp. 1–6, IEEE, 2022.
- [15] J. Izykowski, E. Rosolowski, P. Balcerek, M. Fulczyk, and M. M. Saha, "Accurate noniterative fault-location algorithm utilizing two-end unsynchronized measurements," *IEEE transactions on power delivery*, vol. 26, no. 2, pp. 547–555, 2009.
- [16] F. Costa, C. Neto, S. Carolino, R. Ribeiro, R. Barreto, T. Rocha, and P. Pott, "Comparison between two versions of the discrete wavelet transform for real-time transient detection on synchronous machine terminals," in *2012 10th IEEE/IAS International Conference on Industry Applications*, pp. 1–5, IEEE, 2012.
- [17] D. B. Percival and A. T. Walden, *Wavelet methods for time series analysis*, vol. 4. Cambridge university press, 2000.
- [18] R. S. Stanković and B. J. Falkowski, "The Haar Wavelet Transform: Its Status and Achievements," *Computers & Electrical Engineering*, vol. 29, no. 1, pp. 25–44, 2003.
- [19] G. Luz, D. Junior, and S. Junior, "HVDC Transmission Line Modeling Analysis in PSCAD and ATP Programs," in *XIII Symposium of Specialists in Electric Operational and Expansion Planning*, 2014, (in Portuguese).
- [20] L. M. Ribeiro, G. A. Cunha, E. P. Ribeiro, A. G. Britto, and F. V. Lopes, "Analysis of traveling waves propagation characteristics considering different transmission line emtp models," in *2020 Workshop on Communication Networks and Power Systems (WCNPS)*, pp. 1–6, IEEE, 2020.
- [21] J. R. Marti, "Accurate modelling of frequency-dependent transmission lines in electromagnetic transient simulations," *IEEE Transactions on power apparatus and systems*, no. 1, pp. 147–157, 1982.
- [22] L. C. Z. Júnior, *Electromagnetic Transients in Power Systems Vol. 52. EdUSP*, 2003, (in Portuguese).